AIAA Guidance, Navigation, and Control (GNC) Conference
August 19-22, 2013, Boston, MA
AIAA 2013-5253

# Operational Capabilities of a Six Degrees of Freedom Spacecraft Simulator

K. Saulnier[*], D. Pérez[†], G. Tilton[‡], D. Gallardo[§], C. Shake[**], R. Huang[††], and R. Bevilacqua [‡‡]
*Rensselaer Polytechnic Institute, Troy, NY, 12180*

**This paper presents a novel six degrees of freedom ground-based experimental testbed, designed for testing new guidance, navigation, and control algorithms for nano-satellites. The development of innovative guidance, navigation and control methodologies is a necessary step in the advance of autonomous spacecraft. The testbed allows for testing these algorithms in a one-g laboratory environment, increasing system reliability while reducing development costs. The system stands out among the existing experimental platforms because all degrees of freedom of motion are dynamically reproduced. The hardware and software components of the testbed are detailed in the paper, as well as the motion tracking system used to perform its navigation. A Lyapunov-based strategy for closed loop control is used in hardware-in-the loop experiments to successfully demonstrate the system's capabilities.**



## Nomenclature

| | | |
|---|---|---|
| $\bar{\boldsymbol{A}}$ | = | reference model dynamics matrix |
| $\bar{\boldsymbol{B}}$ | = | control distribution matrix |
| $\boldsymbol{d}_{x,y,z}$ | = | moment arms of the thrusters |
| $\boldsymbol{e}$ | = | tracking error vector |
| $\bar{\boldsymbol{H}}$ | = | thrust distribution matrix |
| $m$ | = | mass of spacecraft |
| $\bar{\boldsymbol{P}}$ | = | solution to the Lyapunov equation |
| $\bar{\boldsymbol{Q}}$ | = | selected matrix for the Lyapunov equation |
| ${}^{I}\bar{\boldsymbol{R}}_{B}$ | = | rotation matrix from the body to the inertial frame |
| $\boldsymbol{u}$ | = | binary thrusts vector |
| $u$ | = | thrust force of a single thruster |
| $\boldsymbol{v}_{\rho l}, \boldsymbol{v}_{\sigma l}$ | = | input to the linear reference model |
| $\boldsymbol{w}$ | = | ideal control vector |
| $V$ | = | Lyapunov function |
| $\boldsymbol{\sigma}$ | = | attitude vector |
| $\boldsymbol{\rho}$ | = | position vector |

[*] Graduate Student, Department of Electrical, Computer, and Systems Engineering, 110 8th Street Troy NY JEC Room 1034. Email: saulnk@rpi.edu
[†] Ph.D. Candidate, Mechanical, Aerospace and Nuclear Engineering Department, 110 8th Street Troy NY JEC Room 1034,AIAA Student Member, Email: perezd3@rpi.edu.
[‡] Student, Mechanical Aerospace and Nuclear Engineering Department, 110 8th Street Troy NY JEC Room 1034. Email: tiltog@rpi.edu
[§] Ph.D. Candidate, Mechanical Aerospace and Nuclear Engineering Department, 110 8th Street Troy NY JEC Room 1034, AIAA Member, Email: gallad3@rpi.edu
[**] Ph.D. Student, Department of Mechanical, Aerospace, & Nuclear Engineering, 110 8th Street Troy NY JEC Room 1034. Email: shakec@rpi.edu
[††] Postdoctoral Research Associate, Mechanical Aerospace and Nuclear Engineering Department, 110 8th Street Troy NY JEC Room 5048, AIAA Member, Email: huangr5@rpi.edu.
[‡‡] Assistant Professor, Mechanical Aerospace and Nuclear Engineering Department, 110 8th Street Troy NY JEC Room 5048, AIAA Member, Email: bevilr@rpi.edu. www.riccardobevilacqua.com

## I. Introduction

THIS paper presents a demonstration of the operational capabilities of the ADvanced Autonomous MUltiple Spacecraft laboratory (ADAMUS lab) 6 degrees of freedom (6DoF) spacecraft simulator developed at RPI and originally presented in Ref. 1. The development of innovative guidance navigation and control (GNC) strategies for spacecraft maneuvering will increase the efficiency and autonomy of future space missions and also reduce their cost. Air bearing-based spacecraft simulators provide the ability to validate these GNC strategies prior to launch with hardware in the loop; providing operating conditions more similar to those to be encountered in space than those provided by any software simulators. Air bearing-based technology provides near frictionless rotational and translational motion which can be utilized to bring one-g laboratory conditions much closer to those encountered in a micro-gravity environment. These kinds of technologies have been developed over the last 50 years with the intention of reducing the costs associated with the design and validation of GNC strategies for spacecraft. The 6DoF testbed developed at the ADAMUS lab falls within the category of *combination systems* (as defined in Ref. 1), which integrate the capabilities of planar systems and rotational systems. Systems which are classified as only planar or only rotational are still widely used in on-the-ground testing. Examples of these include a rotational testbed at Georgia Tech which is used for attitude matching experiments and a planar testbed at Cornell University called FloatCube which was created specifically for testing small scale cooperative satellite maneuvers[2,3]. Combination systems can have 5 to 6 degrees of freedom by combining a planar translation stage and a rotational attitude stage. The Marshall Space Flight Center's Flight Robotics Laboratory has one of the most advanced simulation platforms of this kind in the world.[4] In this case, 6DoF motion is provided on a flat surface of 44 ft x 66 ft with vertical motion provided by a cylindrical lift and not by thrusters. A 5DoF testbed has been developed by the Lawrence Livermore National Laboratory.[5] It combines a rotational platform with full freedom yaw, ± 15° pitch and ± 30° roll on a dynamic air bearing vehicle but does not have a vertical degree of freedom. More recent research related to 5DoF simulators has been done by Georgia Institute of Technology and Harbin Institute of Technology. Both projects combine a lower platform guaranteeing 2 translational degrees of freedom with an upper platform which uses a spherical air bearing, to provide an additional 3 rotational DoF.[6,7] An interesting example of 6DoF testbed is the MIT "SPHERES" project.[8,9] This testbed can reach full 6DoF when used in the International Space Station (ISS)'s micro-gravity environment. 6DoF platforms have been developed by NASA Jet Propulsion Laboratory and New Mexico State University. In both cases the vertical motion, giving the 6th degree of freedom is provided by a powered vertical system which is actively controlled to provide a simulated zero-g environment for the attitude stage (AS).[10,11]

The main goal of this work is to demonstrate the operational capabilities of the 6DoF testbed developed at the ADAMUS lab. The testbed differs from the existing 6DoF systems because it guarantees a dynamical representation of motion along/about the full 6 degrees of freedom. The resulting behavior of the system is much closer to the actual dynamics that satellites encounter when operated on the field, as compared to systems that use linear motors or other kinematical software-based solutions.

The design of the ADAMUS platform potentially allows for testing different spacecraft by simply switching out the AS. Figure 1 shows the interchangeable attitude stage, connected to the testbed base through the spherical air bearing.

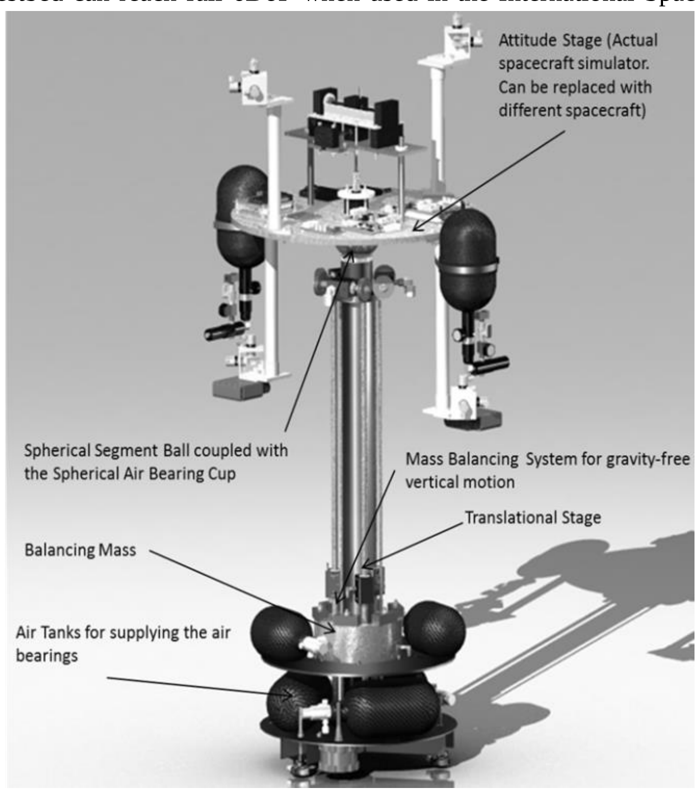

**Figure 1. Attitude Stage connected to the Translational Stage through a spherical air bearing**

An important feature of the ADAMUS testbed is how it directly addresses the challenges of near gravity-free vertical translation in a one-g field. This is accomplished using a unique counterbalance method that employs a matched variable-mass counterbalance and near-frictionless air bearing pulleys to allow close to gravity-free motion along the local gravity vector. The counterbalance system replaces the powered vertical stages of other 6DoF testbeds and allows for control of all 6DoF using only the onboard thrusters.

The overall system represented in Figure 1 operates on a flat epoxy surface. The position and attitude of the testbed is provided in real time by the PhaseSpace Impulse System® (PhaseSpace System), a motion capture system which streams tracking navigation data to the testbed's onboard computer.

The foremost contributions in this work are:

1) Finalization of the completely dynamic 6DoF testbed hardware.
2) Implementation of Lyapunov-based thruster activation control system on the 6DoF testbed for translational and rotational motions
3) Demonstration of the capabilities of the 6DoF testbed for validating GNC algorithms for spacecraft performing autonomous maneuvers via hardware in the loop experiments.

This work is organized as follows: Section II gives an overview of the 6DoF testbed and presents latest developments, Section III illustrates the navigation method and hardware used for the experiments, Section IV comments on the implemented Lyapunov-based thrusters' controls system, Section V explains the automatic generation of code from Simulink models, used to program the onboard computer, and the GNC experiments that are currently finalized using the 6DoF testbed. Section VI presents the conclusions.

## II. General Overview

The testbed, shown in Figure 1, is composed by a Translational Stage (TS) which was designed by the ADAMUS lab and built by Guidance Dynamics Corporation® (GDC) and by an Attitude Stage (AS), designed and built by the ADAMUS lab. Three linear air bearings create an air cushion between the TS and a 13 ft x 15 ft epoxy floor which allows the TS to translate with very little friction. The epoxy floor, Figure 2, was built by Precision Epoxy Products, a division of Rock Art, Ltd. Along with the air pad feet, the TS carries compressed air tanks to provide air to all air bearings used in the testbed. The AS contains all the major subsystems that would be present in a spacecraft. 12 cold gas thrusters are placed on the AS in order to provide control forces and torques for translational and rotational motions in and around the 3 body axes. Also aboard the AS is a PC104 onboard computer and a linear motor system which is used to control the center of mass. The AS is connected to the TS through a hemispherical air bearing which creates a cushion of air between two concentric curved surfaces to provide low friction rotation around three axes. A system of air pulleys on the TS which connect the central column and AS to a counterbalance deck, allows for gravity-free vertical motion of the AS. The counterbalance deck is equipped with an Arduino Uno and WiFly expansion board to provide wireless communication to the AS. Two compressed air tanks on the counterbalance deck are controlled by the Arduino system to release air throughout each experiment as dictated by the onboard computer located on the AS. The release of air from the counterbalance deck is necessary to compensate for the air which is being released through the thrusters on the AS side of the counterbalance. An onboard computer runs the thruster activation strategy according to the of GNC algorithms to be tested. These algorithms use the navigation information streamed by the PhaseSpace motion capture system. The PhaseSpace motion capture system uses a set

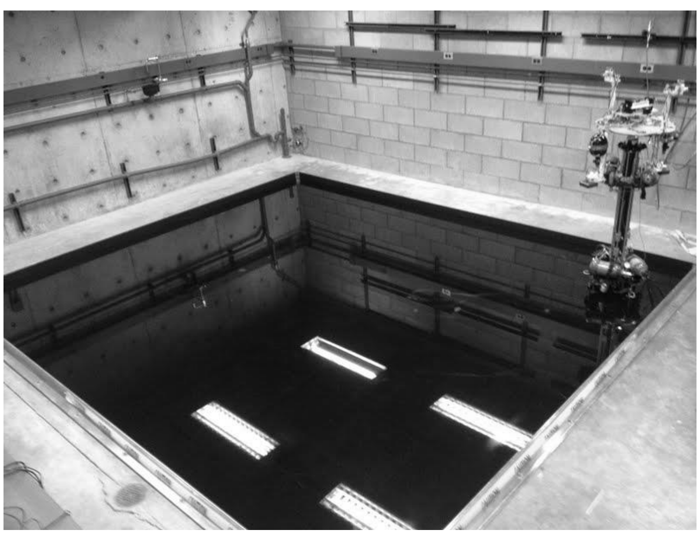

**Figure 2. Epoxy floor.**

of cameras to track LEDs, which are distributed on the AS. From that information, a dedicated server reconstructs the position and attitude of the AS and sends that information to the onboard computer over WiFi. The compressed air used by the thrusters is provided by two tanks attached to the two lower arms of the AS. The electrical power to run the testbed subsystems is provided by two lithium-ion batteries connected to a power management system which is also located on the AS. Table 1 lists the main components of the testbed, and the companies they have been purchased from.

## A. Translational Stage

The function of the TS, as indicated by its name, is to provide the 3 translational degrees of freedom. The TS was custom built by Guidance Dynamics Corporation®, according to the ADAMUS laboratory specifications. Figure 5 shows a rendering and the actual TS. The two horizontal degrees of freedom are provided by air pads which create an air cushion to separate the structure from the epoxy floor allowing for nearly friction free motion.

**Table 1. Testbed Main Components.**

| Element | Assembly | Components | Model | Company |
|---|---|---|---|---|
| Moving Platform | Translational Stage | - | - | Guidance Dynamics Corporation |
| | | Arduino UNO Board | DEV-09950 | Sparkfun |
| | | Venting Electro valve | 23KK7DELM | Peter Paul Electronics |
| | | Pressure Transducer | A-10 | WIKA |
| | | Wifly Shield | WRL-09954 | Sparkfun |
| | Attitude Stage | Thrusters, 12x | EH2012 | Gems Sensors and Controls |
| | | Battery Management System | MP-04R | OceanServer Technology Inc. |
| | | DC-DC Converter | DC123R | OceanServer Technology Inc. |
| | | Li-ion Batteries, 2x | ND2054 | Inspired Energy® |
| | | Tracking System (LEDs and Puck) | PhaseSpace Impulse System | PhaseSpace Inc. |
| | | Compressed Air Tanks, 2x | Ninja 4550 | Ninja Paintball |
| | | Relays Module | IR104-PBF | Diamonds Systems |
| | | Wireless Receiver | DWL-G730AP | D-Link |
| | | Onboard Computer | ADLS15PC | Advanced Digital Logic |
| | | Pressure Transducer | A-10 | WIKA |
| | | Motor Controller Card | DCM-2133 | Galil Motion Control |
| | | Motor Drives | SDM-20242 | Galil Motion Control |
| | | Non-Captive Motor (2) | 35F4N-2.33-024 | Haydon Kerk |
| | | Captive Motor | 35H4N-2.33-049 | Haydon Kerk |
| Epoxy Floor | - | - | - | Precision Epoxy Products |
| Tracking Apparatus | - | Camera, Server, Wireless devices | PhaseSpace Impulse System | PhaseSpace Inc. |

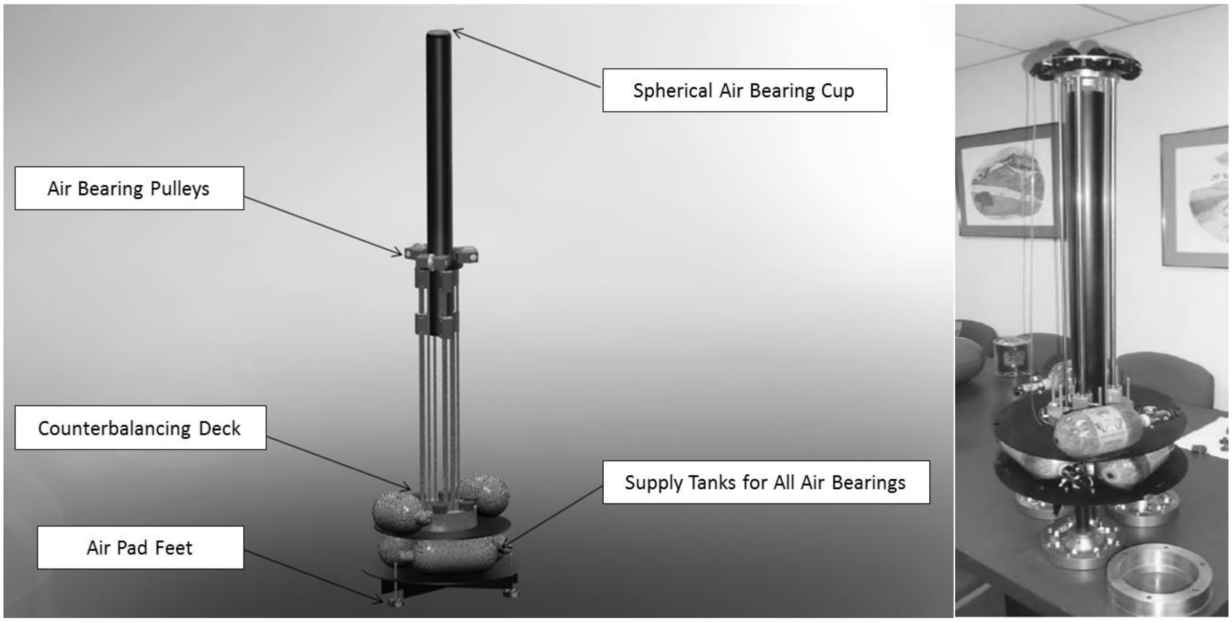


**Figure 5. Translational Stage, a) Rendering b) Actual Picture**

The vertical degree of freedom is provided by a counterbalancing system based on air pulleys. The system consists of a counterbalancing deck of the same mass as the AS and supporting column. The counterbalancing system, shown in Figure 3 and Figure 4, carries two compressed air tanks which match the tanks on the AS which provide fuel to the thrusters. As the AS tanks empty the mass of the stage changes by ~300 g. The counterbalance deck uses its tanks to dynamically adapt its mass to AS. Before each experiment, the tanks of the counterbalancing deck and the matching thruster tanks on the AS are precisely filled with the same amount of air using pressure transmitters to measure the pressure of each set of tanks. Any change in the air contained in the AS tanks translates into a pressure drop. The pressure transmitter on the AS is connected to the onboard computer through a peripheral I/O board. Over the course of an experiment, pressure readings are taken from the AS tanks and streamed over WiFi to a Arduino UNO board and WiFly expansion board, which are located on the counterbalancing deck. The tanks located on the counterbalancing deck are monitored by a pressure transmitter connected directly to the Arduino Uno. The two pressure signals are compared and if the counterbalance stage is higher pressure, Arduino will lower the air content on the counterbalancing deck by activating a venting magnetic latching valve connected to the counterbalancing deck tanks. The venting valve is closed by the Arduino as soon as the pressure difference between the tanks goes to zero. The air released from the counterbalancing deck is released at a single point perpendicular to the vertical motion. This configuration prevents the force from the released air from affecting the vertical motion.

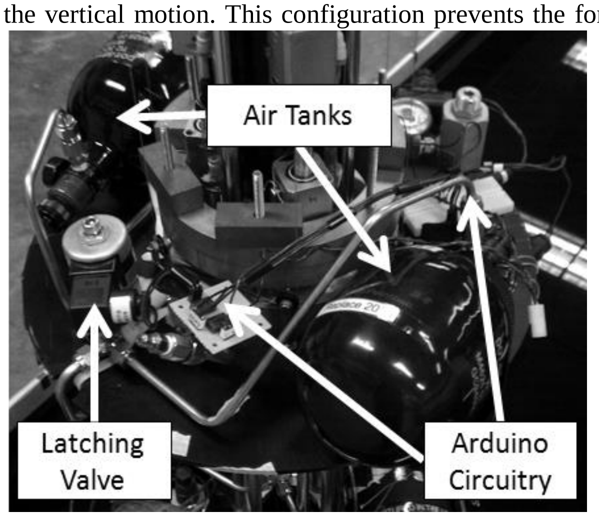


**Figure 3: Counterbalancing Deck**

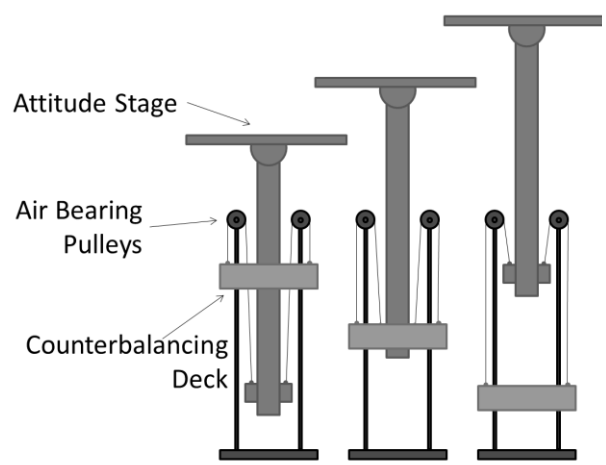


**Figure 4: Representation of the counterbalance system.**

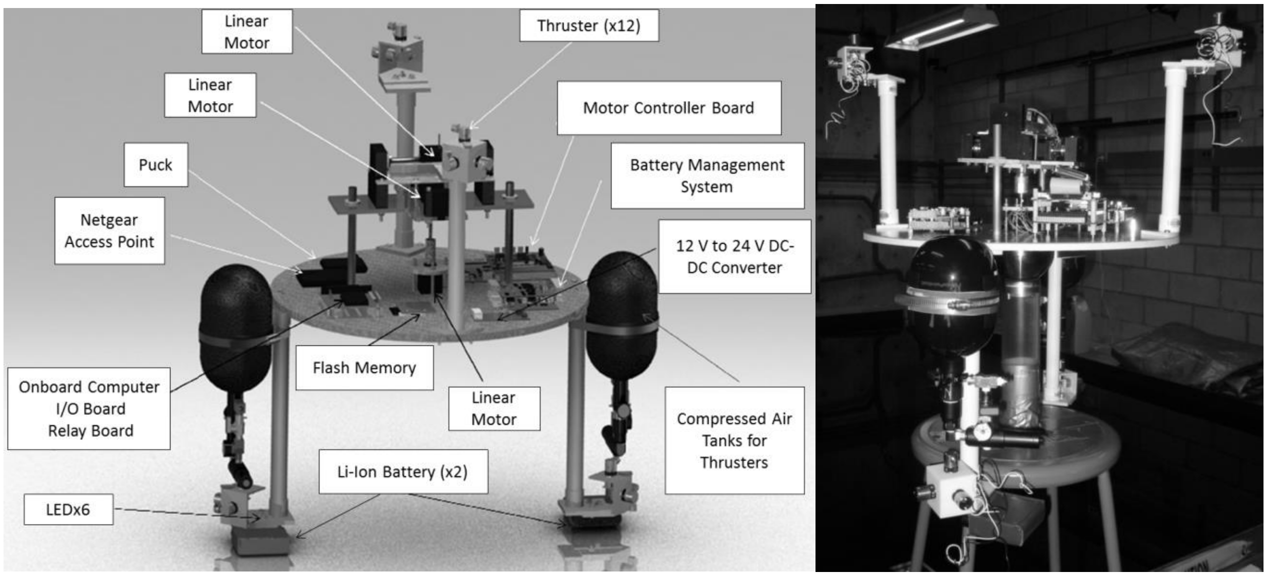


**Figure 6. Attitude Stage a) Rendering b) Actual Picture.**

The downside to the configuration is that it causes the TS to spin. Since the hemispherical air bearing between the TS and the AS is nearly friction free, this has only small effects on the motion of the AS representing the satellite. The counterbalance electrical systems are powered by 9V batteries for the Arduino and 6V lithium ion batteries for the magnetic latching valve.

The TS ends with a hemispherical air bearing cup which supports the mating hemispherical segment ball which is attached to the AS. The TS also carries the compressed air tanks and interconnected pneumatics that store and distribute the air used by all the air bearings of the platform.

### B. Attitude Stage

The AS is composed of a disc made of composite material (fiber glass and high density foam) connected to the hemispherical air bearing. Attached to the AS are four ABS arms. Two arms extend upwards and the other two arms extend downwards. The arms are attached symmetrically to the disc to facilitate mass balancing and proper propulsion when the thrusters are activated. There are three thrusters mounted orthogonally on the end of each arm. Using the proper combination of active thrusters it is possible to obtain independent translational and/or rotational motions. The AS provides full 360° freedom in yaw and ± 30° about the pitch and roll axes. The thrusters are fed with compressed air, which is stored in carbon fiber tanks attached to the AS. During the simulation operations there is a constant mass loss due to the compressed air usage, therefore the tanks are placed having their combined center of mass coincident with the center of rotation of the attitude stage. The flat disk of the AS also supports the power management system, the onboard computer, and the PhaseSpace puck. The puck is a device used by the PhaseSpace Impulse System® for powering and controlling the LEDs necessary to determine the position and attitude of the AS. A total of 6 such LEDs are positioned on the edges of the arms and on the middle of the upper platform. The batteries needed to power the rest of the AS electrical system are located on the lower arms in order to compensate for the mass of the systems above the platform. Figure 6 a) and b) show the AS connected to the air bearing but detached from the TS in a render and actual view respectively. Wiring and pneumatic connections are not shown in the pictures to improve clarity.

An important problem when dealing with rotational testbeds is the need to align the center of mass and center of rotation to eliminate gravity torques. The center of rotation of the AS is located in the center of the hemispherical air bearing that it rotates around. Rough balancing of the AS is done with the addition of any major hardware on the platform. The rough balancing is done with static weights placed in four locations around the AS platform. Due to the movement of small masses such as wires and the need to remove parts for charging and repairs, a fine active mass balancing system called the Balancing Platform (BP) is also present on the AS. The BP consists of three linear motors which translate along the three body axes. The motor's translation causes a shift in the center of mass of the AS. Current balancing techniques are human-in-the-loop with the motors controlled via a motor driver board with a serial connection to the onboard computer. It is also possible to align the center of mass and the center of rotation using adaptive methods. Using these methods the masses are moved until the equilibrium position is reached, where

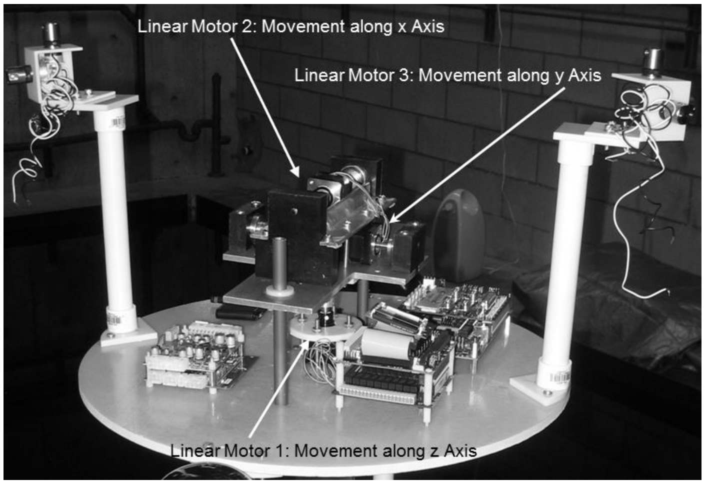


**Figure 7. Magnified view of the Balancing Platform connected to the Attitude Stage through Linear Motor 1.**

the center of mass is aligned to the center of rotation of the joint.[12,13] A close up of the BP prior to the completion of the AS systems can be seen in Figure 7. This early version is shown for clarity.

### C. Power and Data Management Subsystems

All of the AS subsystems, except the PhaseSpace puck and LEDs, rely on 2 lithium-ion batteries for power. These batteries are connected to a Power Management System from Ocean Server Technology (IBPS: Intelligent Battery and Power System). This system is extremely versatile and is able to: 1) recharge the batteries when connected to the 120V grid using a safety charging circuit, and 2) provide the required power at several voltages. The IBPS provides 5V power to the onboard computer (Advanced Digital Logic ADLS15PC Rev. 1.3) and 12V power to a separate 12V to 24V DC-DC converter. The IBPS also provides power to the motor driver and motor controller card. The 12V to 24V DC-DC converter outputs 24V to a relay module which is used to power the thrusters. The relay module is also connected to the onboard computer which can send open or close each relay and thus control the electrical connection of each thruster's electro-valve. The signal sent to the relays can be generated in real time according to the GNC algorithm being run on the system.

The onboard computer is also used to direct the motor controller card used to move the motors on the BP. This operation of calibration is done which human-in-the-loop in a setup phase, before each GNC experiment, so that the experiments may begin on a completely balanced platform. The ADAMUS laboratory is also developing algorithms that will allow continuous balancing of the platform during the experimental phase (during the testing of GNC) since small variations of the position of the center of mass could provoke undesired gravity torques, which could

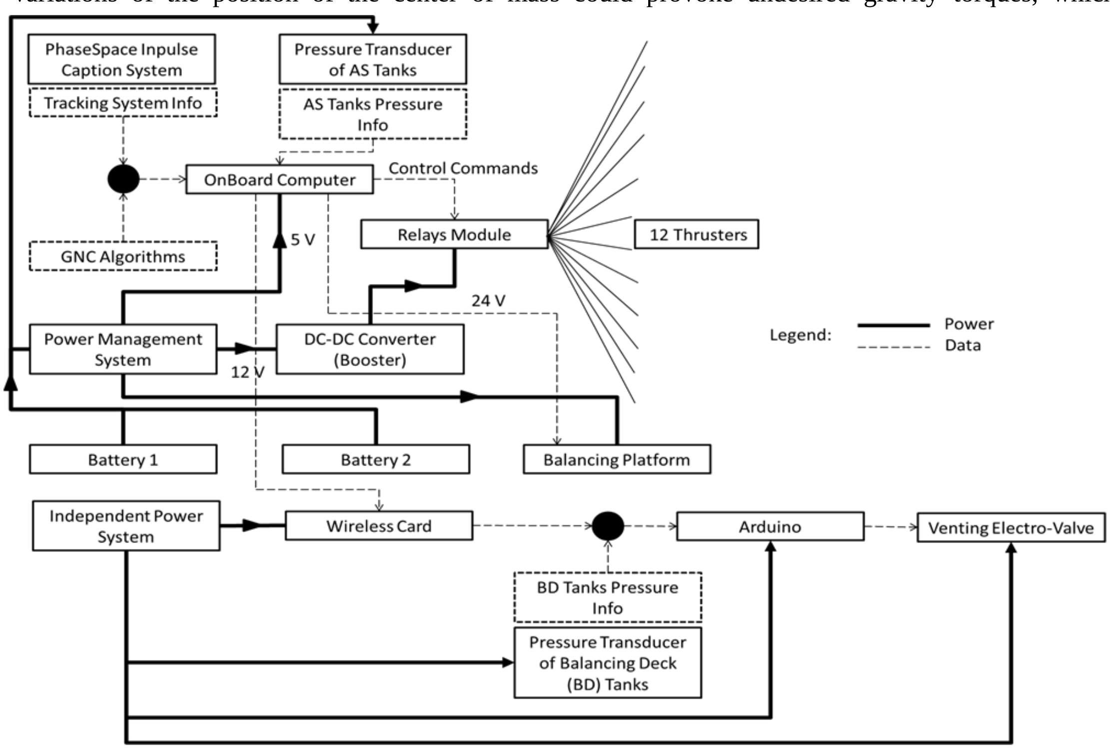


**Figure 8. Electrical connections and signals.**

compromise the simulated zero-g conditions. The onboard computer also collects pressure data coming from a pressure transmitter connected to the air tanks and streams it wirelessly to a wireless card located on the balancing deck on the TS. The Arduino board and the wireless sensor are powered by an independent power system consisting of lithium-ion batteries located with them on the counterbalancing deck. Figure 8 illustrates the scheme of the electrical connections and the signals in the system.

## III. 6DoF Testbed Navigation

The 6DoF testbed is equipped with the PhaseSpace Impulse System® (PhaseSpace System), a motion capture system which determines both position, and attitude. The PhaseSpace System (which is further explain below) outputs a state vector that contains the absolute position of the AS in millimeters, referenced from one of the corners of the epoxy floor, and quaternions representing the attitude of the AS. This data is sent wirelessly to the onboard computer where an executable real time program can use it to generate the linear and angular velocities using a Kalman filter and extended Kalman filter respectively.

A PhaseSpace motion capture system consists of a set of cameras mounted on the walls around the test area and a number of red LEDs mounted on the object to be tracked, providing an easily configurable system that can be used to track any object without requiring extensive calibration or data post-processing. PhaseSpace has software available to run on a desktop that receives data from the system and can show a live representation of the LED locations on the screen, and also provides lower-level software libraries to make the data available to other applications. Those libraries have been used by ADAMUS lab to create S-functions allowing the PhaseSpace data to be collected and used by MATLAB in Simulink and real time executables created using the Simulink Coder[14].

### A. Hardware

A dedicated server computer communicates over Ethernet with each of the PhaseSpace cameras posted around the epoxy floor to obtain positional data from each and compute the tracking information. Each of the cameras consists of two linear pixel arrays set at 90 degrees to each other, each 45 degrees to the vertical, allowing the system to quickly determine the LED position in the 2D camera plane without needing to search a full 2D image. This method significantly increases the tracking speed while minimizing the processing power required. The LEDs are connected to a small battery pack called the puck, mounted on the tracked object. The puck includes a wireless link to the PhaseSpace computer which allows it to conserve power and turn the LEDs off when data isn't being requested. Each puck can power and control up to 72 LEDs which are all connected to a single two-wire cable, allowing easy placement around the tracked object. The LEDs blink rapidly in unique patterns to identify themselves to the cameras, providing clean data without the risk of point swapping and jumps in the output data.

### B. Software

PhaseSpace provides a fully-featured software package for a computer to connect to the server. This software includes a program to show a graphical representation of all LEDs being tracked in the test area and contains various options for data export. While this is a useful debugging and configuration tool, the majority of the data acquisition for the ADAMUS lab is done through the C++ API. A communications library is available for Linux (and other operating systems) which can be used in Simulink S-functions. A PhaseSpace block for Simulink was developed in the lab and is used in all the models where positional information is desired. The block outputs a single 7-element vector of the position and quaternion for the tracked object, as calculated by the PhaseSpace server based on the geometric information of the LEDs locations in the object coordinate frame. The relative LED locations are hard-coded into the S-function because the AS geometry is constant, but the array is easily modified, to accommodate any changes which require the LEDs to be repositioned.

The position data is sent through a Kalman filter in order to smooth the data and to determine the velocity. Similarly the attitude data is sent to an extended Kalman filter which smooths the attitude data. The angular velocity data is computed using a discrete derivative of the filtered attitude data which is passed through a low pass filter to decrease noise. The filter is chosen to balance the speed of the filter and the noise rejection. The results of the filtering process can be seen in Figure 9 compared with a position and attitude signal generated in Simulink using the Aerospace Blockset 6DoF dynamics block.

## IV. Lyapunov Controller for Thrusters

The control strategy for the testbed is adapted from the Lyapunov thruster selection approach described in Ref. 15. The active thrusters are chosen at each time step to maintain a negative derivative to a Lyapunov function created with the linear reference model, thus ensuring stability of the tracking error. The Lyapunov method of

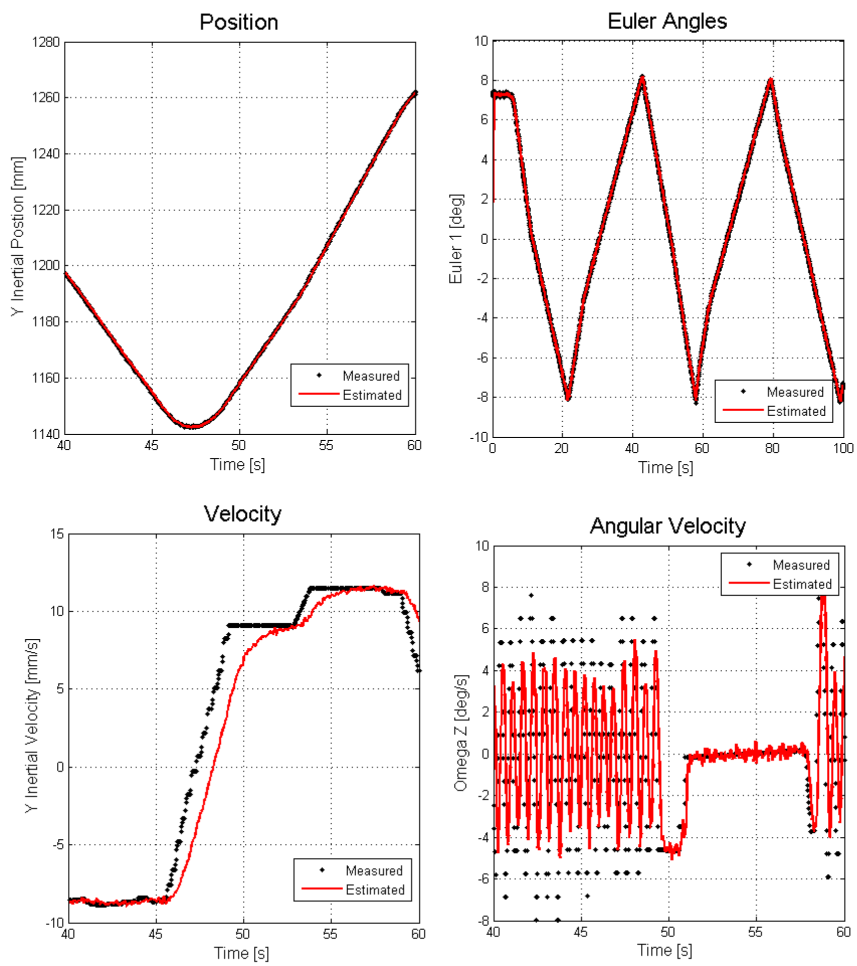


**Figure 9: Results of the Kalman filter and derivative filtering.**

selecting thrusters eliminates the need for thruster mapping and provides a computationally simple, and non-iterative, method for providing a guaranteed feasible 6DoF trajectory.

## A. Linear Reference Model

A linear reference model is defined for the purpose of creating a candidate Lyapunov function. The differential equations for linear dynamics (as shown in Eq. (1)) are used to create the reference model.

$$\ddot{\boldsymbol{\rho}}_{\boldsymbol{d}} + \overline{\boldsymbol{K}}_{\mathbf{1}}\dot{\boldsymbol{\rho}}_{\boldsymbol{d}} + \overline{\boldsymbol{K}}_{\mathbf{2}}\boldsymbol{\rho}_{\boldsymbol{d}} = \boldsymbol{v}_{\boldsymbol{\rho c}} \qquad \ddot{\boldsymbol{\sigma}}_{\boldsymbol{d}} + \overline{\boldsymbol{K}}_{\mathbf{3}}\dot{\boldsymbol{\sigma}}_{\boldsymbol{d}} + \overline{\boldsymbol{K}}_{\mathbf{4}}\boldsymbol{\sigma}_{\boldsymbol{d}} = \boldsymbol{v}_{\boldsymbol{\sigma c}} \tag{1}$$

$\boldsymbol{\rho}_{\boldsymbol{d}}$ and $\boldsymbol{\sigma}_{\boldsymbol{d}}$ represent the translational and rotational motion with respect to a reference frame. $\boldsymbol{v}_{\boldsymbol{\rho c}}$ and $\boldsymbol{v}_{\boldsymbol{\sigma c}}$ represent the input vectors for the translational and rotational motion. The matrices $\boldsymbol{K}_{\boldsymbol{i}}, \boldsymbol{i} = \mathbf{1}, \mathbf{2}, \mathbf{3}, \mathbf{4}$ are gain matrices which are chosen to ensure the stability of the system. Equation (1) can be represented in state space form

$$\dot{\boldsymbol{x}}_{\boldsymbol{d}} = \overline{\boldsymbol{A}}\boldsymbol{x}_{\boldsymbol{d}} + \overline{\boldsymbol{B}}\boldsymbol{u}_{\boldsymbol{d}}, \tag{2}$$

where $\boldsymbol{x}_{\boldsymbol{d}} = [\boldsymbol{\rho}_{\boldsymbol{d}} \quad \boldsymbol{\sigma}_{\boldsymbol{d}}]^T$ and $\boldsymbol{u}_{\boldsymbol{d}} = [\boldsymbol{v}_{\boldsymbol{\rho c}} \quad \boldsymbol{v}_{\boldsymbol{\sigma c}}]^T$ and

$$\overline{\boldsymbol{A}} = \begin{bmatrix} 0_{3x3} & I_{3x3} & 0_{3x3} & 0_{3x3} \\ -\overline{\boldsymbol{K}}_{\mathbf{1}} & -\overline{\boldsymbol{K}}_{\mathbf{2}} & 0_{3x3} & 0_{3x3} \\ 0_{3x3} & 0_{3x3} & 0_{3x3} & I_{3x3} \\ 0_{3x3} & 0_{3x3} & -\overline{\boldsymbol{K}}_{\mathbf{3}} & -\overline{\boldsymbol{K}}_{\mathbf{4}} \end{bmatrix} \overline{\boldsymbol{B}} = \begin{bmatrix} 0_{3x3} & 0_{3x3} \\ I_{3x3} & 0_{3x3} \\ 0_{3x3} & 0_{3x3} \\ 0_{3x3} & I_{3x3} \end{bmatrix}. \tag{3}$$

### B. Lyapunov Based Thruster Selection

A matrix $\boldsymbol{\bar{H}}$ is created representing the contribution of each thruster to the torques and forces in the body frame of the AS. The $\boldsymbol{\bar{H}}$ matrix is customized to the thruster configuration of the AS. The $\boldsymbol{\bar{H}}$ matrix for the simple thruster configuration shown in Figure 10 is shown in Eq. (4).

$$\boldsymbol{\bar{H}} = \begin{bmatrix} \boldsymbol{\bar{H}}_F \\ \boldsymbol{\bar{H}}_M \end{bmatrix}$$

$$\boldsymbol{\bar{H}}_F = \begin{bmatrix} -1 & 0 & 0 & -1 & 0 & 0 & 1 & 0 & 0 & 1 & 0 & 0 \\ 0 & 1 & 0 & 0 & -1 & 0 & 0 & 1 & 0 & 0 & -1 & 0 \\ 0 & 0 & 1 & 0 & 0 & -1 & 0 & 0 & -1 & 0 & 0 & 1 \end{bmatrix} \tag{4}$$

$$\boldsymbol{\bar{H}}_M = \begin{bmatrix} 0 & d_z & -d_y & 0 & d_z & -d_y & 0 & -d_z & d_y & 0 & -d_z & d_y \\ d_z & 0 & -d_x & -d_z & 0 & d_x & d_z & 0 & -d_x & -d_z & 0 & d_x \\ -d_y & d_x & 0 & d_y & -d_x & 0 & d_y & -d_x & 0 & -d_y & d_x & 0 \end{bmatrix}$$

$d_{x,y,z}$ represent the moment arms of the thrusters with respect to the center of rotation of the AS. The first column of $\boldsymbol{\bar{H}_F}$ can be interpreted as thruster 1 contributing force in the –x direction as can be seen in Figure 10. The $\boldsymbol{\bar{H}}$ matrix allows for the input to the system to be represented as

$$\boldsymbol{u_d} = [\boldsymbol{\bar{H}_F} \ \ \boldsymbol{\bar{H}_M}]^{\boldsymbol{T}}\boldsymbol{u}, \tag{5}$$

where $\boldsymbol{u}$ is a 12x1 vector such that the value $u_i = 0$ indicates that thruster $i$ is OFF and $u_i = u$ indicates that thruster $i$ is ON and thrusting with its full force $u$.

A candidate Lyapunov function is then chosen in the form

$$V = \boldsymbol{e^T}\boldsymbol{\bar{P}}\boldsymbol{e} \qquad \boldsymbol{\bar{P}}_{12x12} > \boldsymbol{0}, \tag{6}$$

where $\boldsymbol{e}$ is the error vector defined as

$$\boldsymbol{e} = \boldsymbol{x} - \boldsymbol{x_d}, \tag{7}$$

In which $\boldsymbol{x}$ is the current state of the system and $\boldsymbol{x_d}$ is a desired final state or trajectory. The matrix $\boldsymbol{\bar{P}}$ is computed by solving the quadratic Lyapunov equation

$$\boldsymbol{\bar{A}^T}\boldsymbol{\bar{P}} + \boldsymbol{\bar{P}}\boldsymbol{\bar{A}} = -\boldsymbol{\bar{Q}}, \tag{8}$$

where $\boldsymbol{Q}$ is chosen to be positive definite and $\boldsymbol{\bar{A}}$ is taken from a model representing the difference between the linear reference model and the nonlinear system $\boldsymbol{\dot{\xi}} = \boldsymbol{\bar{A}}\boldsymbol{\xi} + \boldsymbol{B}(\boldsymbol{\bar{H}^T}\boldsymbol{u} - \boldsymbol{w})$.

Here $\boldsymbol{w}$ is a term which contains all the nonlinear terms in the error system.

The time derivative of the Lyapunov function is taken, resulting in the equation

$$\dot{V} = \boldsymbol{e^T}(-\boldsymbol{\bar{Q}})\boldsymbol{e} + 2\boldsymbol{e^T}\boldsymbol{\bar{P}}\boldsymbol{\bar{B}}(\boldsymbol{\bar{H}^T}\boldsymbol{u} - \boldsymbol{w}), \tag{9}$$

The only term in Eq. , (9) that can be modified by the thruster values is the second term

$$2\boldsymbol{e^T}\boldsymbol{\bar{P}}\boldsymbol{\bar{B}}([\boldsymbol{\bar{H}_F} \ \ \boldsymbol{\bar{H}_M}]^{\boldsymbol{T}}\boldsymbol{u}), \tag{10}$$

so at each time step $\boldsymbol{u}$ is chosen such that the term in

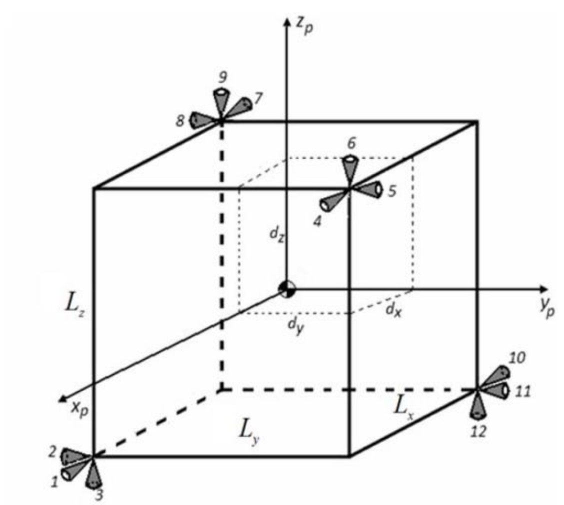


**Figure 10. Thruster configuration on the testbed.** [15]

Eq. (10) is negative. As opposed to the method in Ref. 15 which selects the thrusters to force the term negative though a series of iterative logical statements, the modified version of the controller creates $\boldsymbol{u}$ using the equation

$$\boldsymbol{u} = u\left[\frac{\boldsymbol{a}-|\boldsymbol{a}|}{2\boldsymbol{a}}\right], \quad \boldsymbol{a} = \boldsymbol{e}^{\boldsymbol{T}}\overline{\boldsymbol{P}}\overline{\boldsymbol{B}}\overline{\boldsymbol{H}}, \quad a \neq 0, \qquad (11)$$

This results in the 12x1 thruster vector $\boldsymbol{u}$ with $u_i = 0$ or $u_i = 1$ depending on whether thruster $i$ is designated OFF or ON. Equation , (11) represents the most general case of the iterative logical control solution presented in Ref. 15. In that reference, the thruster selection method was validated for a 3DoF simulation and experiment as well as a 6DoF simulation. Implementation of this modified control on the testbed serves to confirm the numerical results from Ref. 15 as well as demonstrate the capabilities of the testbed.

## V. 6DoF Testbed GNC Experiments

### A. Experiments

The 6DoF testbed hardware and GNC systems was be tested by performing hardware-in-the-loop experiments. These experiments validate the ability of the testbed to accurately simulate complex spacecraft autonomous maneuvers, which allows for the validation of novel GNC algorithms, starting with the Lyapunov approach described in the previous section.

The first class of experiments consists of having the AS move to given state. In other words, starting from a given initial position and attitude, the AS will be forced to reach a desired position and/or attitude without the path being specified (no guidance). This is accomplished by using the Lyapunov based thruster selection as a regulator. These experiments corroborate the control strategy stability and to assess the performance of the navigation system.

### B. Simulink Model

Matlab Simulink is used to implement the control strategy as well as handle the navigation systems and control the thruster relays. The Simulink model, shown in Figure 11, is used to generate C code which can be compiled and run on the onboard Linux computer. The onboard computer and a desktop computer which runs Matlab and Simulink both use an Real Time Application Interface (RTAI) Linux. The RTAI operating system was chosen because it allows the applications to run in real time without being interrupted by operating system tasks. The main blocks in the model are the Sensor Package, State Estimator, Lyapunov Controller, and Diamond Relay Board. The Sensor Package block contains the PhaseSpace System block created in the ADAMUS lab to communicate with the PhaseSpace server and to output the current position and attitude of the AS. This block also has the capability of being used in simulation via a global variable switch which changes the block to use the Simulink built in 6DoF dynamics block to propagate the position and attitude. The State Estimator block contains a Kalman filter and extended Kalman filter which are used to reduce noise and account for lapses in data due to the PhaseSpace System or wireless connection, and also serve to estimate velocity and angular velocity information from the position and attitude information. The Lyapunov Controller block contains the implementation of the Lyapunov based thruster selection which is described in Section IV. The output of the Lyapunov Controller block is the 12x1 vector $\boldsymbol{u}$**,** which contains 1's for the thrusters which should be turned ON and 0's for the thrusters which should be kept or turned OFF. The Diamond Relay Board block operates the onboard relays using the output of the control block. The block Save collects the data held to be held in RAM until then end of an experiment when it is saved to the onboard flash hard drive. The data is taken from the hard drive back to a desktop computer running Linux and Matlab so the data can be plotted and analyzed.

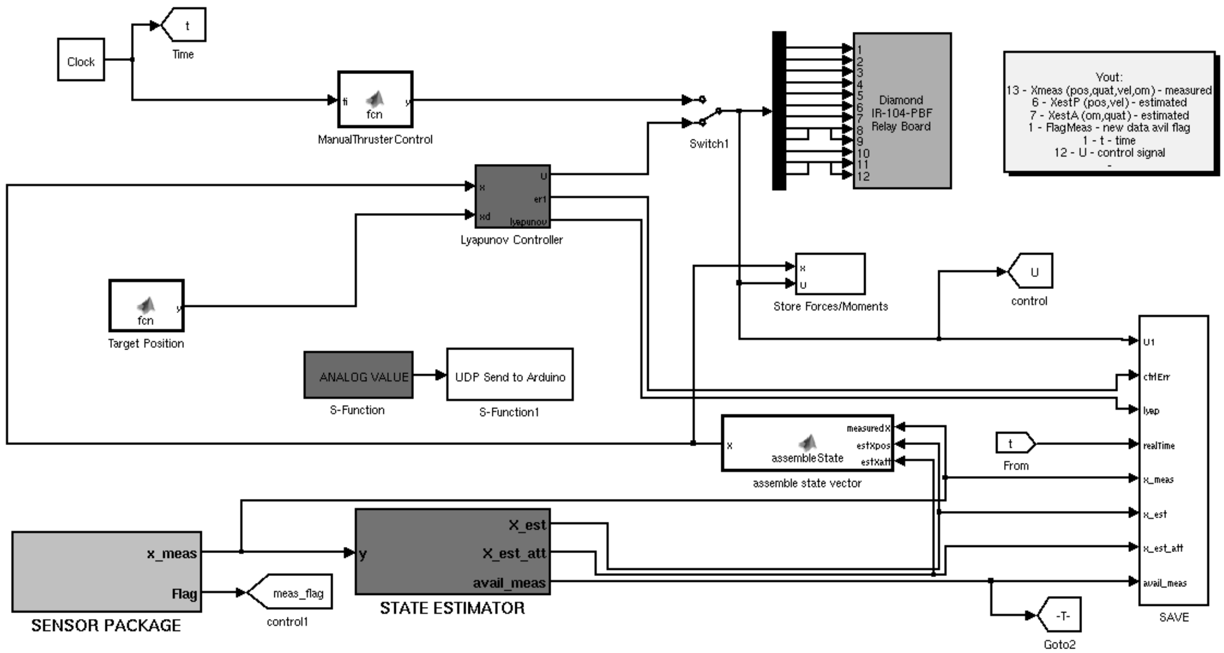


**Figure 11: The Simulink model used for both experiments and simulation.**

### C. Results

Experiments were run starting at an arbitrary initial condition with the testbed floating freely but not moving on the epoxy floor. The testbed software represented in Figure 11 was then run causing the testbed to regulate to a final condition which was preset in the software.

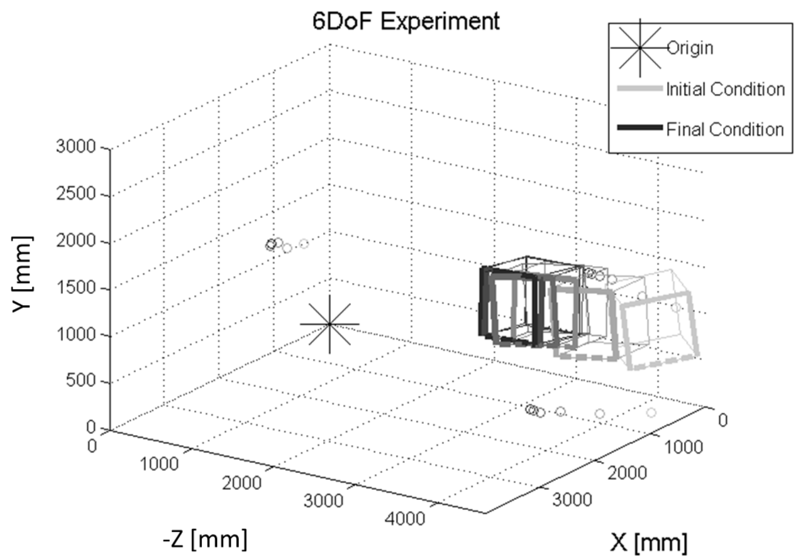


**Figure 13: 6DoF experiment from Figure 12 with the AS represented with a cube.**

The results for regulation in 6DoF are shown in Figure 12 and can be seen in video online[§§]. It can be seen that along the three axes in position the control is able to move from the initial to the final condition. The same can be seen in the Euler angles. There is a threshold for position and attitude which allows small errors to be ignored to prevent chatter at steady state. For position this threshold in 5 cm and the effects cannot be seen in the plots in Figure 12. For attitude the threshold used was 8°. Euler angle 1 and 3 are near or under this threshold for the entire experiment which can be seen in the movement to and from the goal line when under 8° which is not caused by thrusters but instead caused by small imbalances in the AS. Euler angle 2, representing rotation around the vertical axis, repeatedly moves up to the 8° line then is pushed back by the thrusters. This effect is caused by a small amount of torque from friction between the TS cup portion of the hemispherical air bearing and the hemisphere on the AS. The release of air from the counterbalancing deck on the TS causes the TS to spin which manifests itself in a small torque in the positive direction of Euler angle 2. Future work includes modifications to the outlet for the air on the counterbalancing deck to prevent the rotation of the TS. The forces and moments applied to the attitude stage are shown in Figure 14. The forces are represented in the inertial frame. In all cases the thrusters are ON for most of the early stages and then are ON less frequently as the experiment progresses. This thrust configuration is a result of the controller and so different frequencies of actuation should be expected from different controllers when they are tested on the system. This experiment clearly shows the 6DoF capabilities of the testbed as it is able to move from an initial to a final condition in a controlled way in 6DoF.

Further experiments were run which were used to validate the dynamics of the testbed. These experiments were done to compare the experimental results with the simulated results obtained from the 6DoF dynamics block from Simulink's Aerospace blockset and the same initial and final conditions. The results of this experiment can be seen in Figure 15. The simulated and experimental results are very similar to each other in the cases where the thrusters

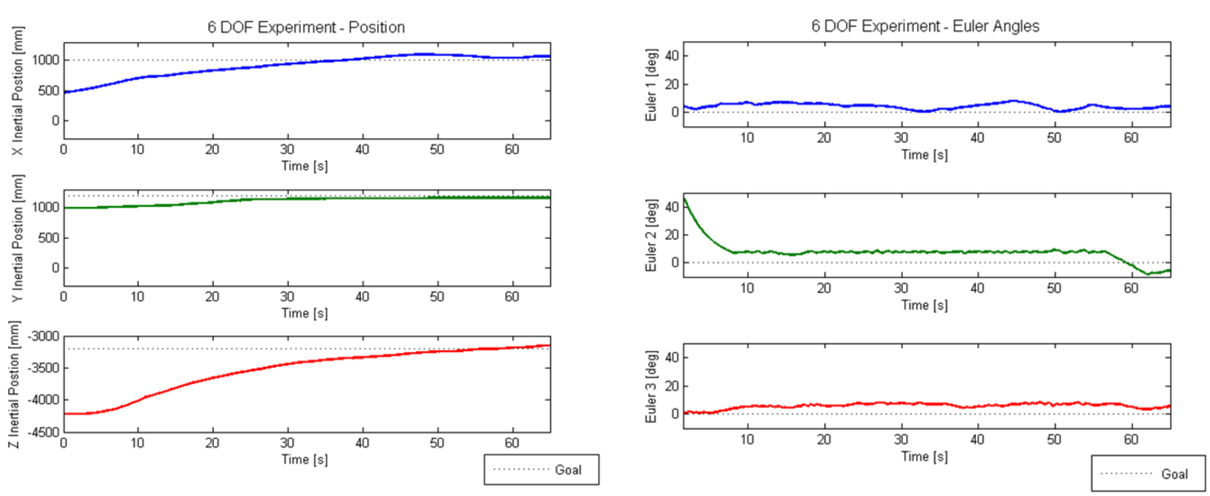


**Figure 12: Results from regulation to a target state (dotted line).**

[§§] Videos of experiments can be seen at: http://www.riccardobevilacqua.com/multimedia.html.

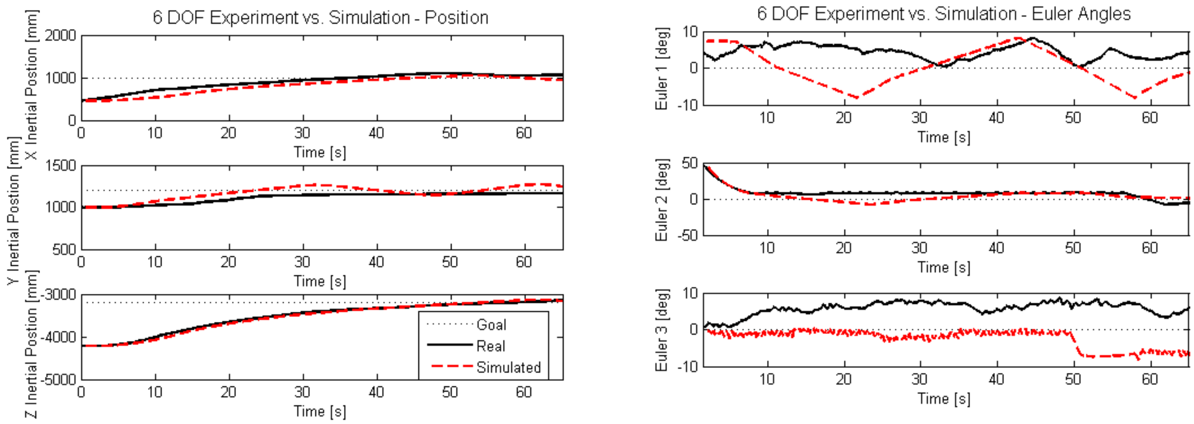


**Figure 15: Simulated results compared with the results from hardware-in-the-loop experiments**

are providing the movement in the hardware-in-the-loop experiments. This is the case for translation and for the vertical axis of rotation (Euler angle 2). The main differences are in Euler angle 2 since the torque from the spinning of the TS is not accounted for in simulation. In vertical translation (Y), the simulation overshoots and the experimental results do not. This is due to friction in the counterbalance system which changes the dynamics of the vertical motion. Some of the friction is due to faulty hardware which will be replaced for future experimental work. The two Euler angles which stay the most time below the threshold are the least similar to the simulation. This is because the main torques affecting their motion when beneath the threshold are the torques caused by imbalances in the testbed AS.

The similarities between the simulated dynamics and system response and the hardware-in-the-loop results further validates the performance of the 6DoF of the testbed.

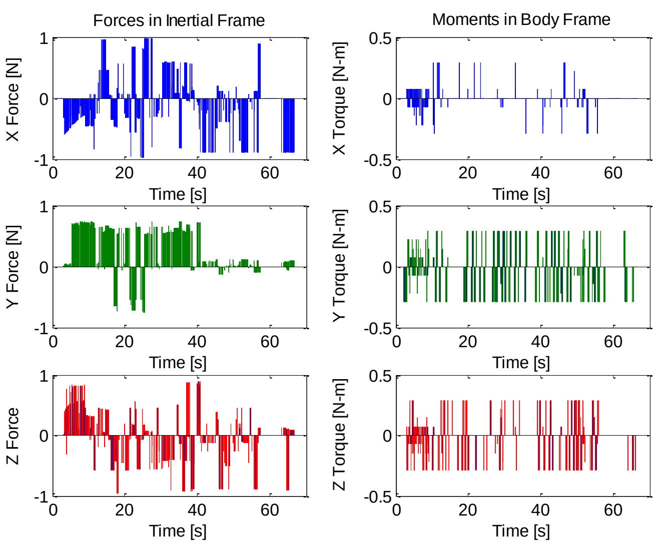


**Figure 14: Forces and moments provided by the thrusters during the 6DoF experiment.**

## VI. Conclusions

The 6DoF spacecraft simulator testbed developed at the ADAMUS laboratory is a unique platform reproducing all degrees of motion in a dynamic fashion. In this work, the hardware and software details of the testbed have been presented, and a Lyapunov-based thruster activation strategy was chosen to demonstrate its capabilities. The experiments for validating the operation of the testbed and for assessing the current navigation and control systems and their possible flaws are described. The results of these experiments confirm the testbed's ability to move and control in 6DoF. A comparison between the dynamics of the testbed and the simulated dynamics show that the two are very similar in cases where the thrusters area actively controlling the testbed. Use of the testbed in validating the Lyapunov-based thruster selection control method demonstrates the utility of the testbed for the design and testing of GNC methodologies. Future work on the testbed will involve the replacement of hardware which is creating friction in the vertical translation as well as modifications to the counterbalance deck to counteract the torque caused by the release of air from the counterbalance compressed air tanks. Further work will also include the testing of additional GNC methods on the current testbed platform and the implementation of balancing software for the AS center of mass alignment with the center of rotation. This will allow the testbed to exhibit the desired dynamics even when not actively controlled by the thrusters.

## References


[1] Gallardo, D., Riccardo, B. and Rasmussen, R. E., "Advances on a 6 Degrees of Freedom Testbed for Autonomous Satellites Operations," *in AIAA Guidance, Dynamics and Control Conference*, AIAA, Washington, DC, 2011.

[2] Jung, J., Park, S., Kim S., Eun, Y. H., and Chang, Y.,"Hardware-in-the-Loop Simulations of Spacecraft Attitude Synchronization Using State-Dependent Riccati Equation Technique," *in Advances in Space Research*, Vol. 51, No. 3, February 2013.

[3] Wilson, W. R., and Peck, M. A., "An air-levitated testbed for flux pinning interactions at the nanosatellite scale," *in AIAA Guidance, Navigation, and Control Conference*, Ontario Canada, August 2010.

[4] Roe, F. D., Mitchell, D. W., Linner, B. M., and Kelley, D. L., "Simulation Techniques for Avionics Systems-An Introduction to a World Class Facility," *in Proceedings of the AIAA Flight Simulation Technologies Conference*, AIAA, Washington, DC, 1996.

[5] Cho, D., Jung, D., and Tsiotras, P., "A 5-DoF Experimental Platform for Spacecraft Rendezvous and Docking," *in Infotech at Aerospace Conference*, AIAA, Washington, DC, 2009.

[6] Jian, X., Gang, B., QinJun, Y., and Jun, L., "Design and Development of a 5-DoF Air-Bearing Spacecraft Simulator," *in Proceedings of the International Asia Conference on Informatics and Control, Automation, and Robotics*, 2009.

[7] Ledebuhr, A., Ng, L., Jones, M., Wilson, B., Gaughan, R., Breitfeller, E., Taylor, W., Robinson, J., Antelman, D. R., and Neilsen, D., ""Micro-Satellite Ground Test Vehicle for Proximity and Docking Operations Development," *in Proceedings of the IEEE Aerospace Conference*, IEEE, Piscataway, NJ, 2001.

[8] Nolet, S., Kong, E. M., and Miller, D. W., "Ground and Flight Testing of Multiple Spacecraft Control on SPHERES During Close Proximity Operations," *Journal of Spacecraft and Rockets*, Vol. 46, No. 6, 2009.

[9] Kong, M., Saenz-Otero, A., Nolet, S., Berkovitz, D. S., Miller, D. W., and Sell, S. W., "SPHERES as a Formation Flight Algorithm Development and Validation Test bed: Current Progress and Beyond," *in Proceedings of 2nd International Symposium on Formation Flying Missions and Technologies*, DLR, Cologne, Germany, 2004.

[10] Regehr, M. W., Acikmese, A. B., Ahmed, A., Aung, M., Clark, K. C., MacNeal, P., Shields, J., Singh, G., Bailey, R., Bushnell, C., Hicke, A., Lytle, B., and Rasmussen, R. E., "The Formation Control Test bed," *in IEEE Proceedings of Aerospace Conference*, IEEE, Piscataway, NJ, 2004.

[11] Viswanathan, S. P., Sanyal, A., Holguin, L., "Dynamics and Control o f a Six Degrees of Freedom Ground Simulator for Autonomous Rendezvous and Proximity Operation of Spacecraft," *in Proceedings of AIAA Guidance, Navigation, and Control Conference*, Minneapolis, Minnesota, 2012.

[12] Kim, J. J., and Agrawal, B. N., "System Identification and Automatic Mass Balancing of Ground-Based Three-Axis Spacecraft Simulator," *in AIAA Guidance, Navigation, and Control Conference and Exhibit*, AIAA, Washington, DC, 2006.

[13] Kim, J. J., and Agrawal, B. N., "Automatic Mass Balancing of Air-Bearing-Based Three-Axis Rotational Spacecraft Simulator," *Journal of Guidance, Control, and Dynamics*, vol. 32, no. 3, pp. 1005-1017, 2009.

[14] Shake, C., Saulnier, K., and Bevilacqua, R., "Spacecraft attitude determination system using nano optical devices and Linux software libraries," *AIAA Journal of Aerospace Computing, Information and Communication*, to appear.

[15] Curti, F., Romano, M., and Bevilacqua, R., "Lyapunov-Based Thrusters' Selection for Spacecraft Control: Analysis and Experimentation," *AIAA Journal of Guidance, Control, and Dynamics*, Vol. 33, No. 4, 2010, pp. 1143-1160.